

Design Considerations for Compressors with Magnetic Bearings

J. F. HUSTAK AND D. J. PEER

Dresser-Rand

Turbo Products Division

P.O. Box 560

Olean, NY 14760

INTRODUCTION

Development of magnetic bearings and dry gas seals has altered the standard design criteria used on centrifugal compressors with conventional oil-film seals and bearings. The authors' company started testing their first oil free compressor in 1979. Since that time much experience has been gained through field operation as shown in Table 1.

RADIAL BEARING SIZE AND SELECTION

Currently, magnetic bearings are being offered as options in units designed for oil-film bearings. Based on the use of conventional ferromagnetic materials, the magnetic bearing projected areas need to be roughly 8 times larger than an oil-film bearing to obtain the same load rating. A magnetic journal bearing would be twice the diameter and four times the length of the oil-film bearing. Higher load ratings are possible by using more expensive magnetic alloys, but the enhancement is usually not cost effective, especially on new equipment where the housing dimensions are somewhat flexible.

The difference in physical size between magnetic bearings and oil-film bearings prompts a more careful look at the actual load requirements of the specific application. The size of the original oil-film journal bearings is based more on shaft design considerations such as torque, flexibility, and neighboring geometry than load rating. So, after determining the static bearing reactions and calculating the maximum dynamic loads, a magnetic bearing load rating is selected based on a suitable service factor.

Calculation of the service loads on the bearing should include some estimation of circumferential pressure gradients. The first and last stages of a multistage unit are particularly susceptible to circumferential pressure gradients because the inlet and discharge geometries are not uniform in the tangential direction. The effects are more severe at the discharge where the gas energy levels are higher. This phenomenon of "radial thrust" is more common in the pump industry, but has been documented in some classic texts on compressors [1]. Traditionally, the problem was associated only with compressors that had cantilevered rotor designs and pump style volute casings, as illustrated in Figure 1.

Circumferential pressure gradients exist in every machine to some degree. Before magnetic bearings, the effects were not observed on multistage centrifugals where the discharge volute is isolated from the impeller by a diffuser passage as shown in Figure 2. Clearly, the loads have been present all along, but the "oversized" oil-film bearings compensated for them.

Figure 3 shows the pressure contours in a vaneless diffuser during aerodynamic testing of a stage similar to Figure 2. The cutwater is that part of the volute where the flow splits between the discharge nozzle and the beginning of the volute. At low capacity, the flow stalls at the volute cutwater and creates a wake in the volute trailing the cutwater. The resulting pressure distribution pushes the impeller toward the low pressure region trailing the cutwater. As the capacity increases, the cutwater flow incidence decreases, the diffuser pressure becomes more uniform, and

the radial thrust load decreases.

By observing the DC currents in each coil, the magnetic journal bearings make it possible to identify the magnitude, direction and location of the radial thrust. When the bearing was designed, the magnetic bearing vendor had envisioned that these currents would be equal and that the static load would be shared by the pair of coils which straddle the vertical centerline in the upper half of the bearing. As shown in Figure 3, the direction of the net static load vector changes. Depending on the volute orientation, the entire static load may shift to one coil (and beyond) as the compressor operating conditions change.

Radial thrust poses no problems for magnetic bearing systems provided that the load rating accounts for it and the system does not rely on the position of permanent magnets to carry the static load.

COMPRESSOR ROTOR

The rotating portion of the magnetic journal bearing is an axial stack of ferromagnetic laminations, designed to eliminate eddy currents in the rotor. The laminations are mounted on a sleeve and shrunk on to the compressor rotor. Typically, the laminated sleeve also includes the position sensor surface which determines the running position of the shaft. The rotor residual unbalance is proportional to the offset between the geometric center of the sensor surface and the rotor's inertial center. For this reason, the laminated bearing sleeves are assembled and ground on the shaft, and the rotor is supported on the sleeve surface during balancing.

API-617 [2] limits the allowable unbalance of centrifugal compressor rotors to $4*W/N$ inch ounces (or $W/(4*N)$ inch pounds), where W is the rotor weight in pounds and N is the maximum speed of the rotor in rpm. By this formula, the allowable eccentricity of the sensor surface is $1/(4*N)$ inches and the allowable runout for a 10,000 rpm unit would be 0.00005 inches, TIR (total indicator reading). Ideally, the outside diameter of the laminated sleeve is kept smaller than the bore of any of the inboard rotor components; such as the seals and impellers. This eliminates the need to remove the bearing sleeves from the shaft. Repeatability of runout on removable sleeves is inadequate to meet the required unbalance levels specified by API.

API has established standards for allowable peak-to-peak vibration levels for shop acceptance testing which were developed based on oil-film bearings. Magnetic bearings are normally softer than oil-film bearings. Consequently, magnetic bearing rotor systems tend to produce more amplitude for the same unbalance; except in the vicinity of response peaks where the decreased bearing/shaft stiffness ratio reduces the amplification factor. Compared to oil-film bearings, magnetic bearings have larger running clearances and different amplitude vs. stiffness characteristics. When the vibration amplitude becomes a significant percentage of the oil-film bearing clearance, the bearing becomes very stiff, and more rotor bending occurs. In a magnetic bearing, high vibration amplitude does not increase the bearing stiffness. Therefore, magnetic bearing vibration amplitude limits must be evaluated in conjunction with shaft deflections and the percentage of available current.

Figure 4 shows magnetic bearing stiffness and damping as a function of frequency [3]. There are narrow frequency ranges where damping values are negligible, and even negative. The bearings will not effectively control any excitation frequency in this range. This results in an amplified and virtually self-sustaining response, dependent on external friction and damping for attenuation. Experience shows that compressors equipped with magnetic bearings exhibit a lower tolerance to incipient surge and sudden changes in operating conditions. Both conditions are accompanied by broad band excitation. The magnetic bearing vendor is careful to design the system characteristics so that these areas of low damping do not coincide with rotor resonances or known excitation frequencies.

664B5/4 MAGNETIC BEARING RETROFIT STUDY

In 1974, four identical 664B5/4 compressors were shipped with five shoe tilt-pad oil bearings and floating ring oil seals. These compressors utilize a back-to-back configuration with five stages in the first section and

four stages in the second section (Figure 5). Although the units successfully completed in-house mechanical testing, subsynchronous instability caused high vibrations in the field. The original bearings and seals were replaced with tilt-pad damper bearings and tilt-pad seals to eliminate the instability problem.

An engineering study was commissioned to determine whether dry gas seals and magnetic bearings would improve mechanical performance and eliminate sour seal oil leakage flow. The re-design required use of the existing casing and as many existing parts as possible.

The first problem encountered was the axial load capability of the magnetic thrust bearing. Rotor dynamic and geometric constraints limited the size of the bearing collar to an outside diameter of 21.0 inches. This corresponds to an effective area of 268 square inches and a load capacity of 18000 lb. The original oil fluid film thrust bearing had an outside diameter of 12.5 in., effective surface area of 75 square inches, and a design axial load capacity of 37500 lb. Thrust load as a function of inlet capacity and speed is shown in Figure 6. Normal design thrust loading ranges from 10000 to 15000 lb. but predicted thrust loads at off-design conditions are as high as 35000 lb. A special thrust unloading device would be required to compensate for any loads greater than 18000 lb.

The rotor dynamic study compared the current oil-film damper bearing/tilt-pad seal rotor configuration to the proposed magnetic bearing/dry gas seal retrofit. Figure 7 shows the differences in undamped critical speeds between the designs. The first mode rigid bearing natural frequency dropped from 2185 cpm on the original to 1711 cpm on the retrofit due to an increase in bearing span. The second and third modes also decreased primarily due to increased overhang weight on the thrust end. The bearing coefficients are plotted on the undamped critical speed map for the current fluid film bearing and the initial magnetic bearing selection. Note that the magnetic bearing/dry gas seal configuration must pass through two natural frequencies during acceleration up to maximum continuous speed. The third mode is within the operating speed range. Past experience has shown difficulties operating close to flexible rotor modes with magnetic bearings. Rawal, et. al. [4], researched the effect of sensor location on the forced response characteristics of rotors with active magnetic bearings. Flexible rotor modes are subject to potential problems when the bearing centerline and probes are at different axial locations.

Synchronous forced response to unbalance analyses were run for both the current oil-film damper bearing/tilt-pad seal and the magnetic bearing/dry gas seal configurations. Figure 8 shows rotor speed vs. amplitude for a coupling unbalance of 1.0 ounce inch. This plot reveals that the third mode amplifies within the operating speed range for the magnetic bearing/dry gas seal configuration. The magnetic bearing/dry gas seal configuration has a sensitivity to coupling unbalance up to two times greater than the damper bearing/tilt-pad design. Figure 9 shows a similar comparison using a thrust collar unbalance of 1.0 ounce inch. Again, the third mode is amplified within the design speed range and a higher sensitivity to unbalance results on the magnetic bearing/gas seal configuration.

Non-removable sleeves were chosen based on a rotor response study which determined the effects of the ferromagnetic sleeve total indicator reading (TIR) runout relative to the shaft inertial center. API allows 1.5 ounce inches per plane unbalance for this rotor at a design speed of 4903 rpm. Since there are two balance planes, a maximum unbalance of 3.0 ounce inches is allowed on the balance machine. Synchronous forced response to unbalance was analyzed with 0.3 ounce inches located at ten equally spaced axial lengths (in phase) along the rotor to simulate a ferromagnetic sleeve runout of 0.1 mils (0.0001 inches) TIR. This resulted in a rotor response of approximately 0.25 mils at the probe locations. The API vibration limit is 1.56 mils, which, assuming no other unbalance, is equivalent to a ferromagnetic sleeve runout of 0.63 mils. This is illustrated in Figure 10. Obviously, a small amount of ferromagnetic sleeve eccentricity results in high vibration readings relative to API limits. The probability of eccentricity between these two pieces increases whenever the sleeve is removed from the shaft; hence the decision to use non-removable ferromagnetic shaft sleeves.

Stability analyses were performed on the following rotor/bearing/seal configurations: (1) original (non-damper tilt-pad bearings/ring seals), (2) current (damper tilt-pad bearings/tilt-pad seals), (3) retrofit (magnetic

bearing/dry gas seals) and (4) an alternative (damper tilt-pad bearings/dry gas seals). The original configuration (1) went unstable in the field. A baseline run was made with this configuration to illustrate the cross-coupling required for instability based on field results. Figure 11 shows that a cross-coupling value of 31,500 lb/in is necessary to drive the original configuration unstable. The predicted aerodynamic cross-coupling is 23,800 lb/in (using a computer program developed by Kirk [5]). Wachel's [5] empirical method for calculating aerodynamic cross-coupling results in a value of 24,300 lb/in.

The current stable configuration (2) installed to correct the original unstable configuration (1) required 54,000 lb/in cross-coupling to drive the system unstable. This set up a baseline design acceptance stability criteria requiring a cross-coupling threshold of 54,000 lb/in. Figure 11 shows that the new retrofit configuration (3) goes unstable at 28,000 lb/in which is below the original (1). An alternative arrangement (4) was considered using oil damper tilt-pad bearings and dry gas seals. This alternative (4) yielded a stability threshold of 67,000 lb./in.; the best of all four designs.

The resultant dynamic stiffness of a magnetic bearing is made up of the vector sum of real (k) and imaginary (Cw) components as shown in Figure 4 (reprinted with permission from reference [3]). Magnetic bearings allow damping adjustments by changing the open-loop phase angle.

To determine the optimum damping value for the magnetic bearing, stiffness was held constant at the first mode forward whirl frequency and damping was varied. Based on stability analysis, damping optimized at approximately 900 lb-sec/in. Even at this level, the stability threshold was predicted at 59,000 lb/in which was not as favorable as the oil tilt-pad damper bearing/dry gas seal configuration (4).

If a stability program is unavailable, an approximate method to determine optimized damping was developed by Barrett, et. al. [7]. Typically, this method yields estimations within fifteen percent of stability analysis results. In this example, the formula below predicted an optimum damping value of 992 lb-sec/in. The equation from reference [7] can be written as follows (valid for flexible shaft systems)[8]:

$$C_o = (1.356 \times 10^{-4}) N_{cr} (M_m + 70417K_b/N_{cr}^2)$$

where:

C_o = Optimum damping, lb-sec/in

N_{cr} = First rigid bearing critical, rpm

M_m = First mode modal mass, lb

K_b = Bearing stiffness at first mode forward whirl frequency, cpm

It is important to optimize damping at the beginning of a rotor dynamic study to reduce the amount of analysis time for a project. Coordination between the bearing supplier and the compressor manufacturer is of utmost importance during the initial design phases.

5P2 MAGNETIC BEARING COMPRESSOR

Four 5P2 magnetic bearing/dry gas seal pipeline compressors have been built and commissioned. There are over forty operating with oil-film bearings. Figure 12 shows the differences in geometry between the two designs.

When magnetic bearings are part of the original equipment, as opposed to retrofits, the designer has greater flexibility. Both an inboard and outboard magnetic thrust bearing were considered in the design of the magnetic bearing system. An inboard magnetic thrust bearing resulted in superior rotor dynamic performance. This configuration also allowed more access for maintenance on the auxiliary ball bearings.

It is a standard practice to compare new designs against designs with successful field operation. Figure 13 shows an undamped critical speed map comparing the differences between an oil-film tilt-pad bearing/dry gas configuration and a magnetic bearing/dry gas seal arrangement. The bearing coefficients are plotted for both the oil-film and the magnetic bearings.

All four of the undamped natural frequencies are lower for the magnetic bearing design. Due to the relative stiffness of the shaft, the first and second modes are critically damped. Experience has also shown that it is possible, and practical, to run on critically damped natural frequencies. Contrary to the previous example, the third mode has a sufficient margin above the operating speed range for both configurations.

Synchronous forced response to unbalance was analyzed for both oil-film tilt-pad bearings/dry gas seals and the magnetic bearing/dry gas seal configurations. A plot of rotor speed vs. amplitude for a coupling unbalance of 1.0 ounce inch is shown in Figure 14. Both configurations have about the same sensitivity to unbalance around the minimum design speed. The magnetic bearing configuration is about twice as sensitive to coupling unbalance at maximum continuous operating speed. This is due to the auxiliary bearing increasing the coupling end overhang. Figure 15 shows a similar comparison using a thrust collar unbalance of 1.0 ounce inch. The inboard thrust collar on the magnetic bearing design decreased the sensitivity to thrust collar unbalance to almost half the oil-film bearing configuration.

Figure 16 plots ferromagnetic sleeve TIR for maximum allowable API unbalance limits. API allows an unbalance of 0.45 ounce inches per plane at a design speed of 7140 rpm. Since there are two balance planes, 0.90 ounce inches would be the allowable unbalance on the balance machine. A synchronous forced response to unbalance analysis was run with 0.09 ounce inches located at ten equally spaced axial lengths (in phase) along the rotor to simulate a ferromagnetic sleeve runout of 0.070 mil TIR. This resulted in a rotor response of approximately 0.031 mils at the probe locations. The API vibration limit is 1.30 mils, which, assuming no other unbalance, is equivalent to a ferromagnetic sleeve runout of 2.94 mils. This compressor is much less sensitive to ferromagnetic sleeve eccentricity compared to the previous example.

Both the oil-film and magnetic bearing designs are exceptionally stable due to the high shaft stiffness. Figure 17 is a stability map showing the threshold of instability at 85,000 lb/in cross-coupling for the magnetic bearing configuration. Wachel's empirical method results in a value of 9,400 lb/in. The magnetic bearing configuration has a stability safety factor greater than 9. The oil-film bearing has an even greater safety factor.

CONCLUSIONS

1. Due to the difference in physical size of the bearings, units with magnetic bearings generally have lower load capabilities.
2. Some operational problems have been experienced when the actual service loads were not sufficiently considered.
3. Mechanical performance acceptability criteria must be expanded to include shaft deflections and bearing load capacity.
4. Sensitivity to runout must be evaluated to determine the acceptability of removable ferromagnetic sleeves.
5. In some circumstances, oil-film bearings provide better performance than magnetic bearings.

REFERENCES

1. Stepanoff, J. A. 1955. Turboblowers, New York, NY, John Wiley & Sons, Inc., pp.162
2. American Petroleum Institute (API) Standard 617, Fifth Edition, April 1988, Washington, D.C., USA
3. Schoeneck, K. A., and Hustak, J. F., 1987. "Comparison of analytical and field experience for a centrifugal compressor using active magnetic bearings." IMechE Paper C104/87. Presented at The Third European Congress Fluid Machinery for the Oil, Petrochemical and Related Industries, The Hague, Netherlands

4. Rawal, D. N., Keese, J. and Kirk, R. G., 1991. "The effect of sensor location on the forced response characteristics of rotors with magnetic bearings." Presented at ROMAG'91, Washington, D.C., USA
5. Kirk, R. G., 1986. "Labyrinth seal analysis for centrifugal compressor design - theory and practice." Presented at the International Conference on Rotordynamics in Tokyo, Japan
6. Wachel, J.C., and von Nimitz, W. W., 1980. "Assuring the reliability of offshore gas compression systems." Paper EUR 205. Presented at the European Offshore Petroleum Conference and Exhibition, London, England
7. Barrett, L. E., Gunter, E. J., and Allaire, P. E., 1977. "Optimum bearing and support damping for unbalance response and stability of rotating machinery." ASME Paper 77-GT-27. Presented at Gas Turbine Conference, Philadelphia, Pa, USA
8. Hustak, J. F., Kirk, R. G., and Schoeneck, K. A., 1986. "Analysis and test results of turbocompressors using active magnetic bearings." Presented at the ASLE 41st Annual Meeting in Toronto, Ontario, Canada

DRESSER-RAND MACHINERY EQUIPPED WITH MAGNETIC BEARINGS
OPERATING HOURS AS OF JANUARY 27, 1992

UNIT/FACILITY	MODEL	ON LINE	HOURS	RPM	APPLICATION
DEVELOPMENT VEHICLE	MTA824BB	1979	1,300	13,000	DEVELOPMENT
NOVA HUSSAR STA.	CDP230	1985	16,375	5,250	NAT. GAS PIPELINE
NOVA KNIGHT #1	1B26	1986	27,353	11,000	NAT. GAS PIPELINE
TRANSCANADA, ONTARIO	CDP416	1986	36,496	14,500	NAT. GAS PIPELINE
SHELL REFINERY	CBF842	1987	32,019	10,250	REFINERY SOUR GAS
NOVA KNIGHT #3	5P2	1988	16,781	7,140	NAT. GAS PIPELINE
NOVA HUSSAR STA.	GT-51	1988	6,434	5,250	POWER TURBINE
NOVA FARRELL LAKE	5P2	1988	17,102	7,140	NAT. GAS PIPELINE
NOVA SCHRADER CREEK #2	5P2	1989	18,022	7,140	NAT. GAS PIPELINE
NOVA DUSTY LAKE	5P2	1989	11,725	7,140	NAT. GAS PIPELINE
NOVA CLEARWATER #1	7.5P1	1989	9,702	5,775	NAT. GAS PIPELINE
NOVA CLEARWATER #5	8.25P1	1990	4,651	5,775	NAT. GAS PIPELINE
NYSEG	DA	1990	7,603	3,600	BOILER FEED PUMP

TABLE 1 - Magnetic Bearing Experience

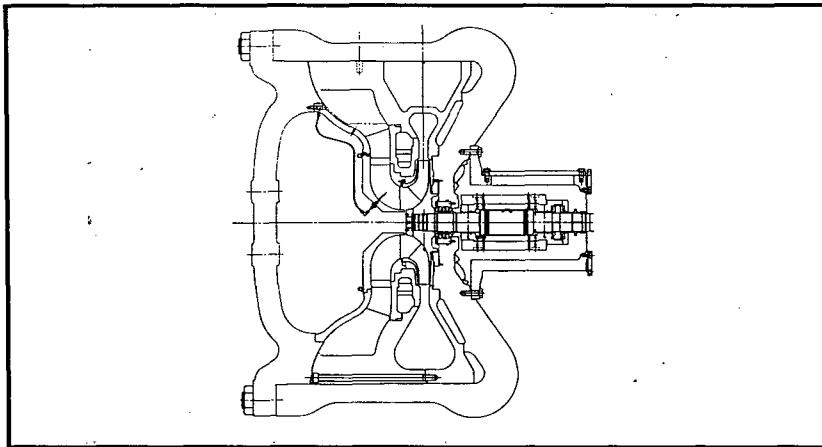


Figure 1 - Single Stage Cantilevered Rotor With Pump Style Volute

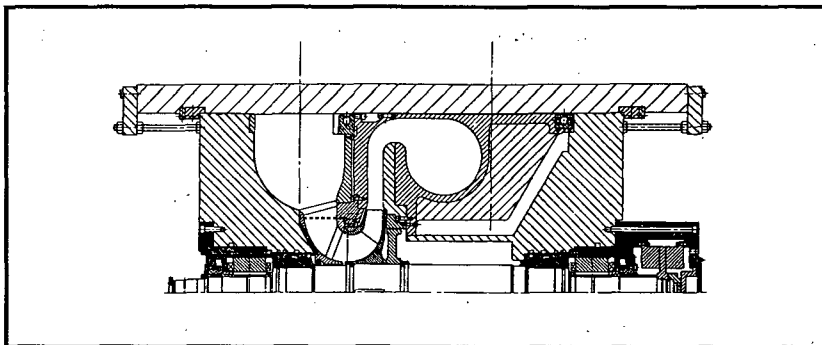


Figure 2 - Single Stage Beam Style Compressor With The Discharge Volute Isolated By A Symmetric Diffuser Passage

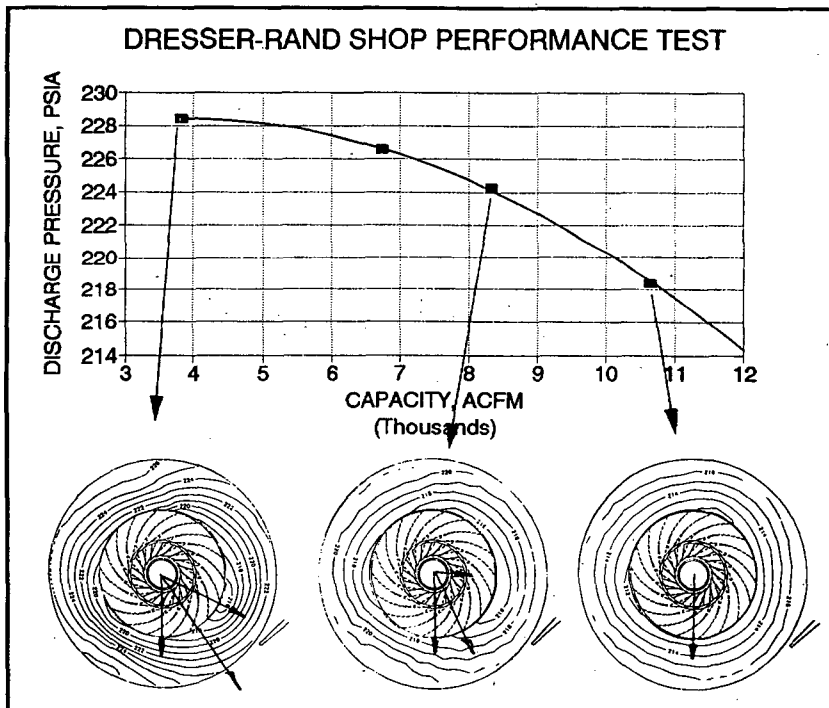


Figure 3 - Pressure Contours In A Vaneless Diffuser

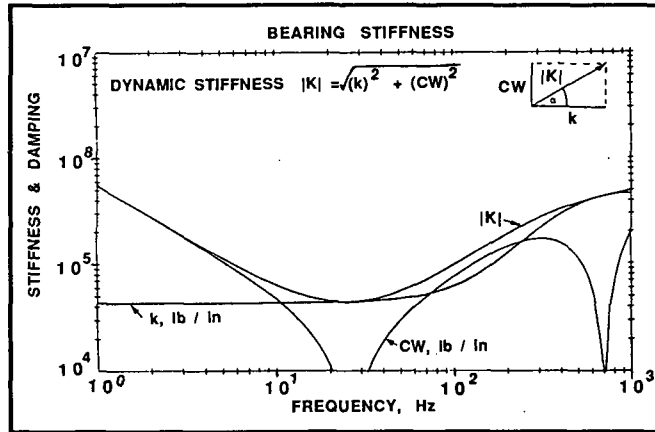


Figure 4 - Magnetic Bearing Stiffness And Damping As A Function Of Excitation Frequency

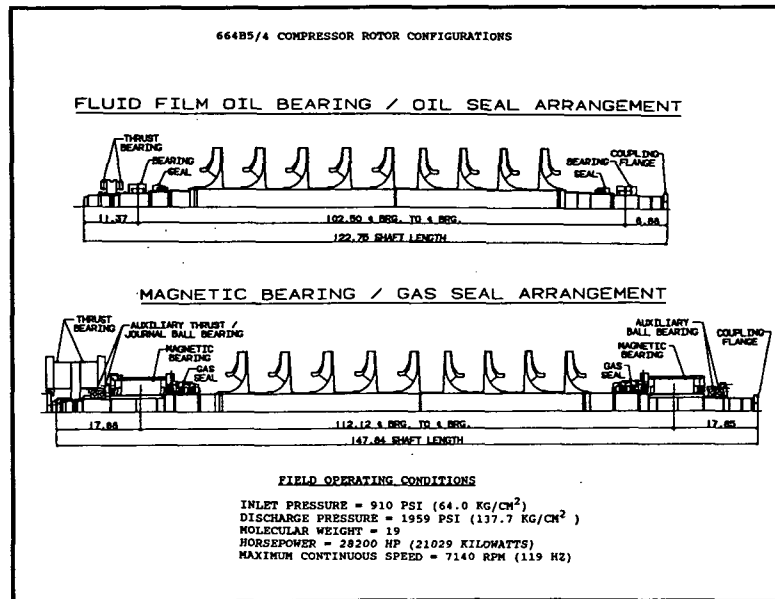


Figure 5 - Comparison Between Oil Fluid Film Bearing / Seal And Magnetic Bearing / Seal Arrangement

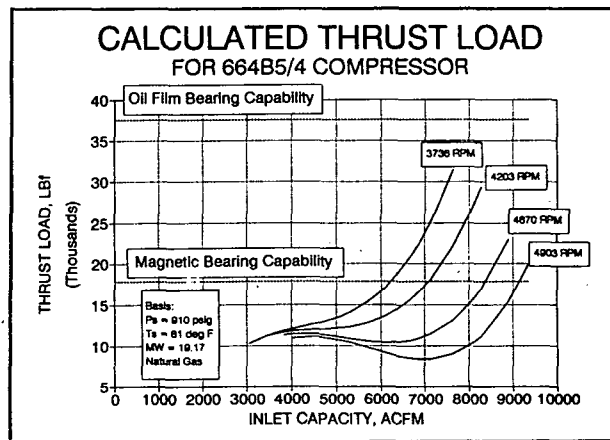


Figure 6 - Calculated Aerodynamic Thrust Load For The 664B5 / 4 Compressor

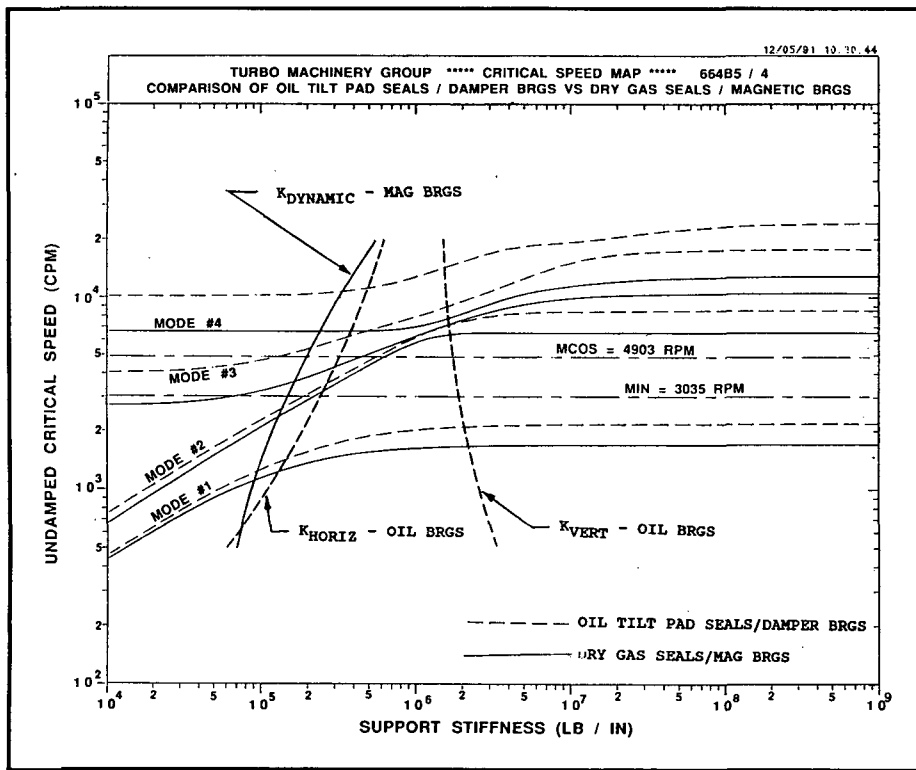


Figure 7 - 664B5 / 4 Undamped Critical Speed Map Comparing Oil Fluid Film Bearing / Seal And Magnetic Bearing / Seal Configurations

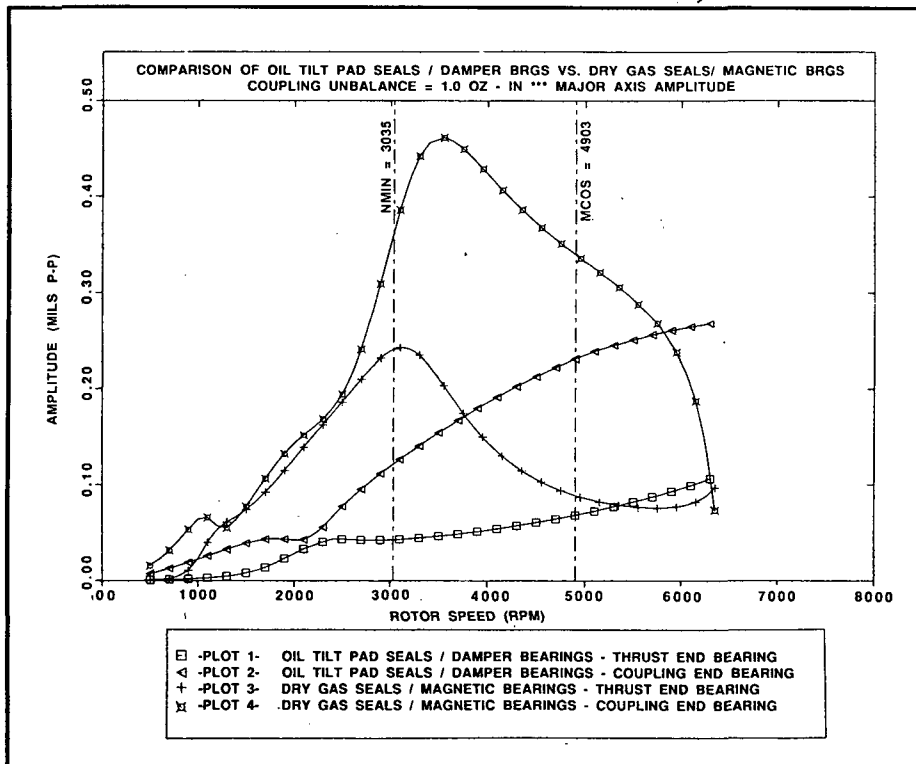


Figure 8 - 664B5 / 4 Synchronous Unbalance Response Using 1.0 Oz - In (0.72 Kg-mm) Coupling Unbalance Comparing Oil Fluid Film Bearing / Seal And Magnetic Bearing / Gas Seal

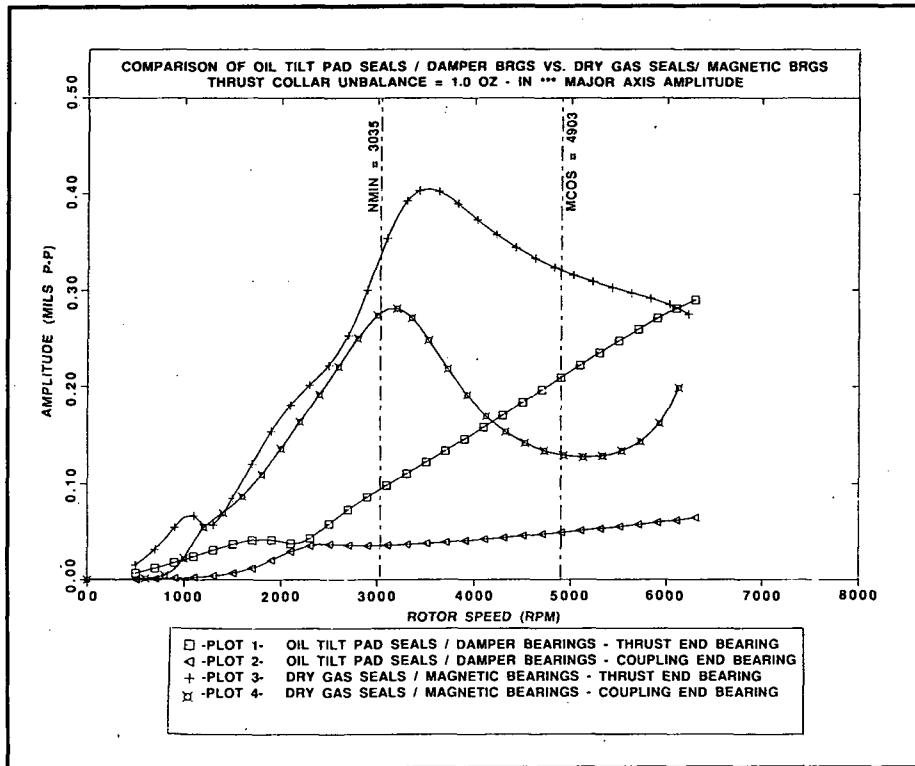


Figure 9 - 664B5 / 4 Synchronous Unbalance Response Using 1.0 Oz - In (0.72 Kg-mm) Thrust Collar Unbalance Comparing Oil Fluid Film Bearing / Seal And Magnetic Bearing / Gas Seal

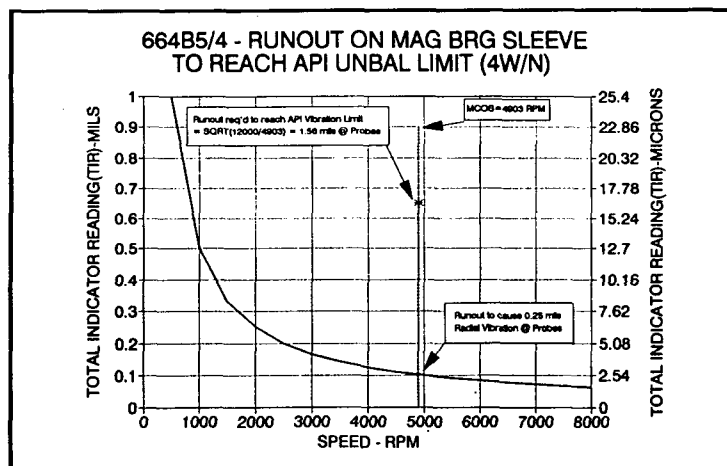


Figure 10 - 664B5 / 4 Runout On Ferromagnetic Sleeve To Reach API 617 Fifth Edition Allowable Unbalance Limits

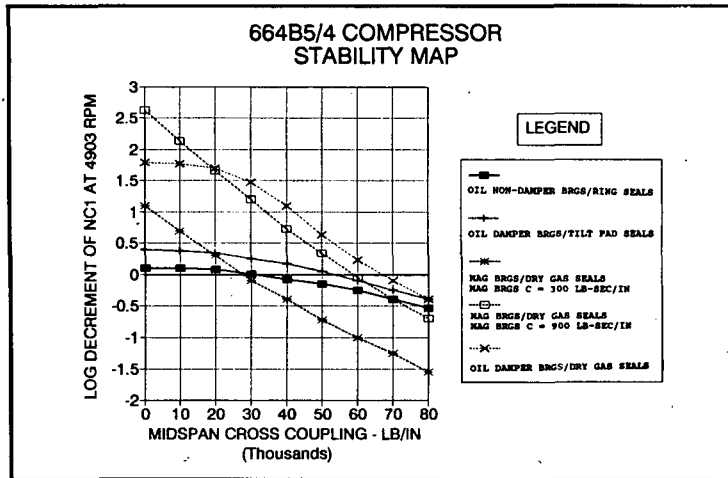


Figure 11 - 664B5 / 4 Stability Map For Various Configurations

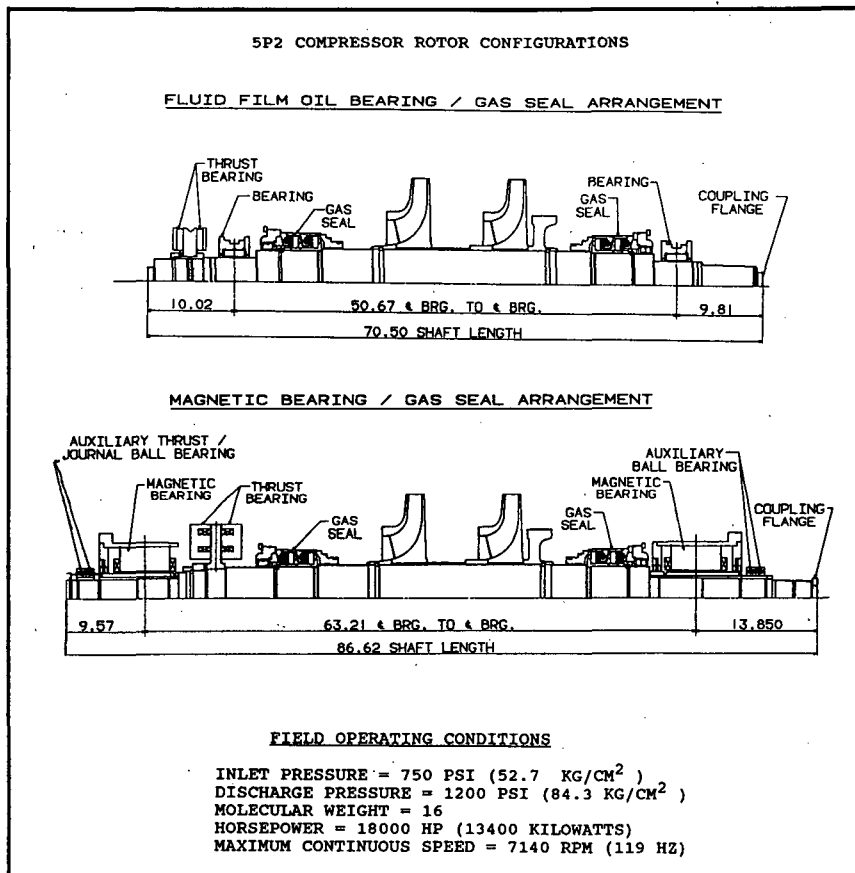


Figure 12 - Comparison Between Oil Fluid Film Bearing / Seal And Magnetic Bearing / Seal Arrangement

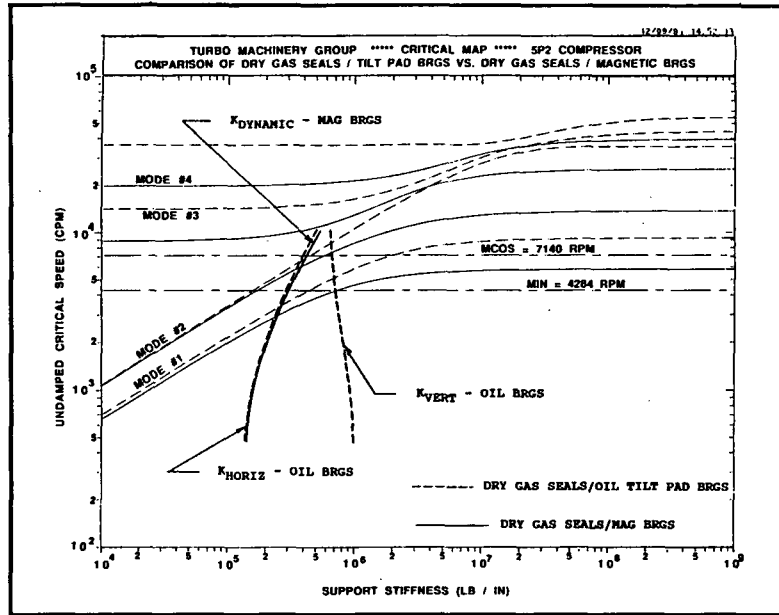


Figure 13 - 5P2 Undamped Critical Speed Map Comparing Oil Fluid Film Bearing / Seal And Magnetic Bearing / Seal Configurations

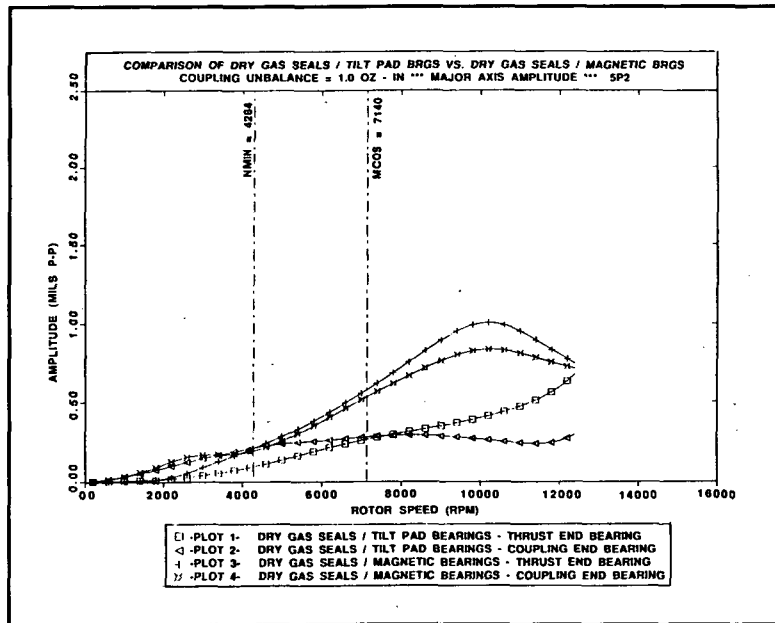


Figure 14 - 5P2 Synchronous Unbalance Response Using 1.0 Oz - In (0.72 kg-mm) Coupling Unbalance Comparing Oil Fluid Film Bearing / Seal And Magnetic Bearing / Gas Seal

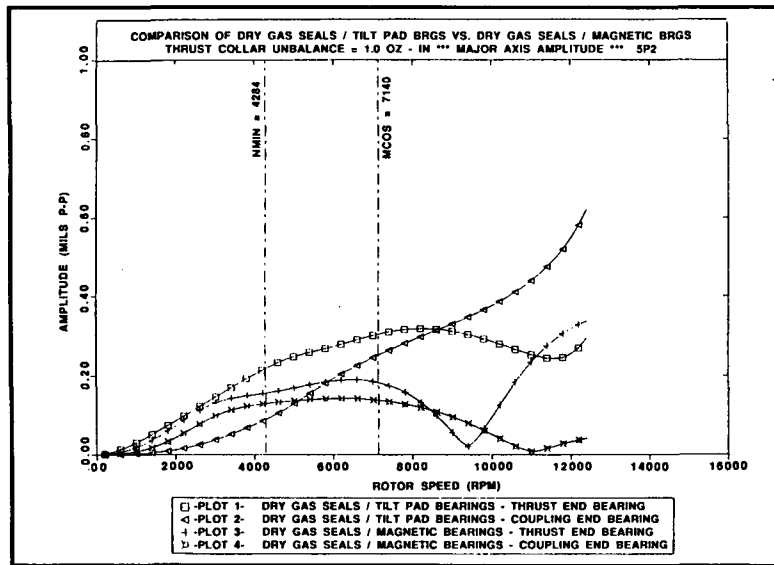


Figure 15 - 5P2 Synchronous Unbalance Response Using 1.0 Oz-in (0.72 Kg-mm) Thrust Collar Unbalance Comparing Oil Fluid Film Bearing / Seal And Magnetic Bearing / Gas Seal

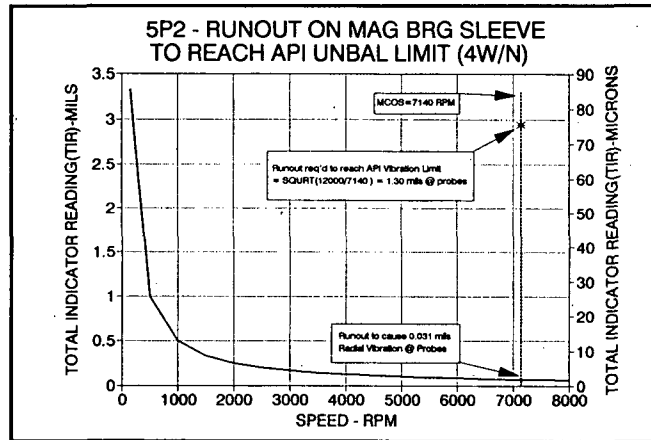


Figure 16 - 5P2 Runout On Ferromagnetic Sleeve To Reach API 617 Fifth Edition Allowable Unbalance Limits

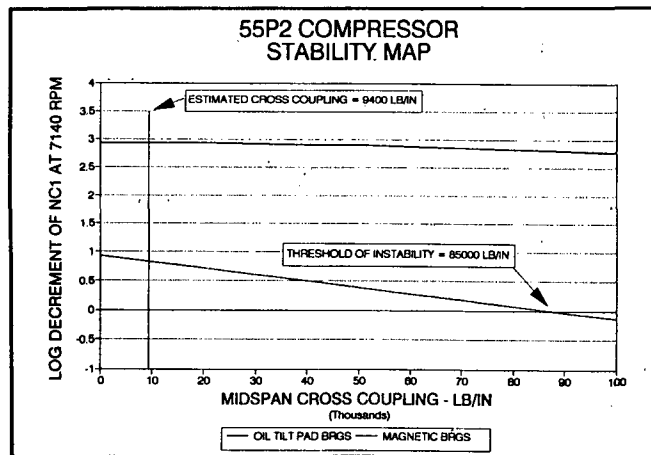


Figure 17 - 5P2 Stability Map For Oil Tilt Pad Bearing And Magnetic Bearing Configurations